Acknowledgments: We thank W. Kaelin for JARID1a antibodies, and *Jarid1a*$^{-/-}$ and *Jarid1a*$^{+/+}$ fibroblasts; and R. Janknecht for JARID1b and JARID1c cDNAs. Supported by NIH grants (EY 16807, DK 091618, and S10 RR027450), the Pew Scholars Program, and a Dana Foundation award to S.P.; a Japan Society for the Promotion of Science fellowship to M.H.; NIH grant F32GM082083 to L.D.; and a Blasker Foundation award to C.V.

Supporting Online Material
www.sciencemag.org/cgi/content/full/333/6051/1881/DC1
Materials and Methods
Figs. S1 to S17
References (*10*–*17*)

24 March 2011; accepted 8 August 2011
10.1126/science.1206022

Superfast Muscles Set Maximum Call Rate in Echolocating Bats

Coen P. H. Elemans,[1]* Andrew F. Mead,[2] Lasse Jakobsen,[1] John M. Ratcliffe[1]*

As an echolocating bat closes in on a flying insect, it increases call emission to rates beyond 160 calls per second. This high call rate phase, dubbed the terminal buzz, has proven enigmatic because it is unknown how bats are able to produce calls so quickly. We found that previously unknown and highly specialized superfast muscles power rapid call rates in the terminal buzz. Additionally, we show that laryngeal motor performance, not overlap between call production and the arrival of echoes at the bat's ears, limits maximum call rate. Superfast muscles are rare in vertebrates and always associated with extraordinary motor demands on acoustic communication. We propose that the advantages of rapid auditory updates on prey movement selected for superfast laryngeal muscle in echolocating bats.

Laryngeal echolocation and insectivory characterize about 70% of present-day bat species (*1*–*3*). Over the course of an attack on a flying insect, bats increase their echolocation call emission rates as they progress from prey detection, through approach, to the terminal buzz (*1*, *2*, *4*) (Fig. 1A). Increasing call emission rates means more information updates per unit time from returning echoes on the relative position of the target. All aerial hawking bats studied to date produce the buzz, which is sometimes subdivided into "buzz I" and "buzz II" phase calls, the former occurring at rates of ~100 to 160 calls/s, and the latter ≥160 calls/s (*1*, *5*) (Fig. 1B). Bats do not call at rates exceeding those reached during this final stage of aerial hawking attack (*2*, *4*), and we hypothesize that call production, echo processing, or both limit maximum echolocation call rate.

Laryngeal nerve-cut experiments reveal that each call a bat emits is under active neuromuscular control (*6*, *7*). Consequently, muscle performance might place an upper limit on the rate at which bats produce calls. Alternatively, if prey echoes overlap with or return after the next call is emitted, accuracy in target ranging may suffer as a result of ambiguity in matching echoes to calls (*1*, *8*). While hunting, most species avoid potential ambiguity by not producing the next call until target echoes reach the bat's ears (*1*), potentially limiting maximum call rates during the buzz. To investigate these hypotheses, we first measured sound production during aerial attack sequences in free-flying Daubenton's bats (*Myotis daubentonii*, Vespertilionidae) using a 12-microphone array (Fig. 1C) (*9*) and determined when the start and the end of each prey echo (Fig. 2, A to C) would impinge upon the bat's ears relative to both the source call and the next call emitted (*10*). Our data show that during a buzz, echoes from individual calls terminate before the start of the next call (Fig. 2C and fig. S1), suggesting no ambiguity in call-echo matching. In fact, for buzz II calls, the repetition rate could theoretically exceed 400 calls/s without any such ambiguity (Fig. 2C and fig. S1), a rate twice as high as the 190 calls/s observed in our study (Fig. 1). Our results also demonstrate that, because call duration decreases during the buzz, there is no overlap between a call and its echo until the bat is less than 5 cm from its target (Fig. 2B), corroborating previous estimates for

[1]Institute of Biology, University of Southern Denmark, DK-5230 Odense M, Denmark. [2]Department of Biology, University of Pennsylvania, Philadelphia, PA 19104, USA.

*To whom correspondence should be addressed. E-mail: coen@biology.sdu.dk (C.P.H.E.); jmr@biology.sdu.dk (J.M.R.)

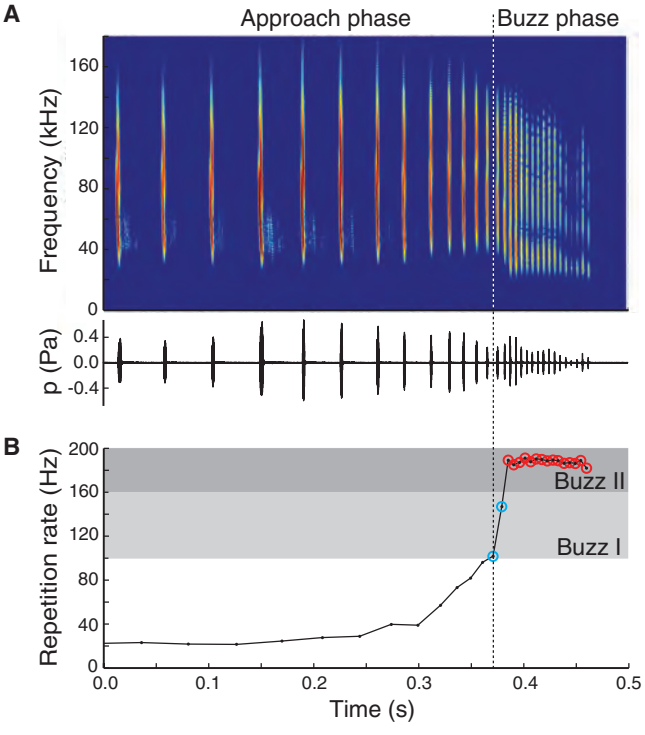

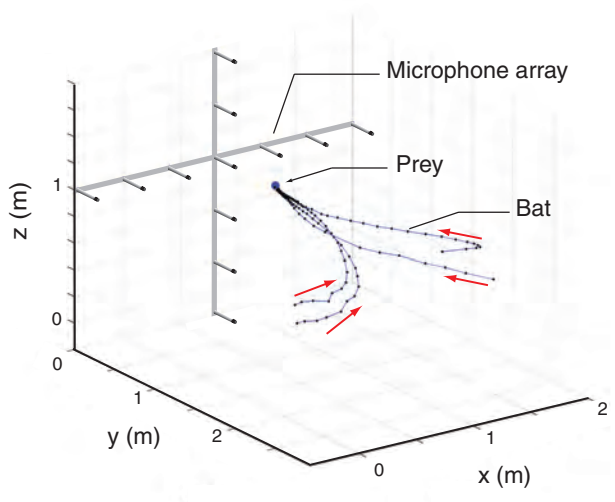

Fig. 1. Echolocation and flight kinematics during aerial attack sequences in *Myotis daubentonii*. (**A**) Spectrogram and oscillogram of emitted echolocation calls as recorded on the center microphone of the array. (**B**) Instantaneous call repetition rates from sequence in (A). The start of buzz I is defined as call repetition rate >100 calls/s (cyan circles, light gray zone). In buzz II, the repetition rate is >160 calls/s (red circles, medium gray zone); here, peak fundamental frequency of the calls drops from 45 to 25 kHz. (**C**) Four reconstructed flight paths from a single bat using a 12-microphone array (*10*). Red arrows indicate flight direction.

this species and others (*1*, *5*, *11*). Assuming a processing time of ~20 ms for each received echo (*12*), any perceptual difficulties created by call-echo overlap at the end of a buzz may be negligible because by the time these echoes have been processed the insect will have already been taken or evaded the bat (*9*). In sum, our data and that of previous reports from the field (*5*) and lab (*11*) indicate that echo processing does not limit call repetition rate in the buzz.

Next, we turned our attention to call production. Vespertilionids and other bat species generate calls in the larynx by flow-induced oscillation of vocal folds (*6*, *7*, *13*, *14*), which terminate as very thin membranes (Fig. 3A). The tension in the folds and membranes determines their oscillation frequency, and thus the frequency of sounds produced. Tension is increased by rotation of the thyroid cartilage around the cricothyroid joint (Fig. 3B) and is mainly controlled by the bat's massive cricothyroid muscle (Fig. 3C). The roles

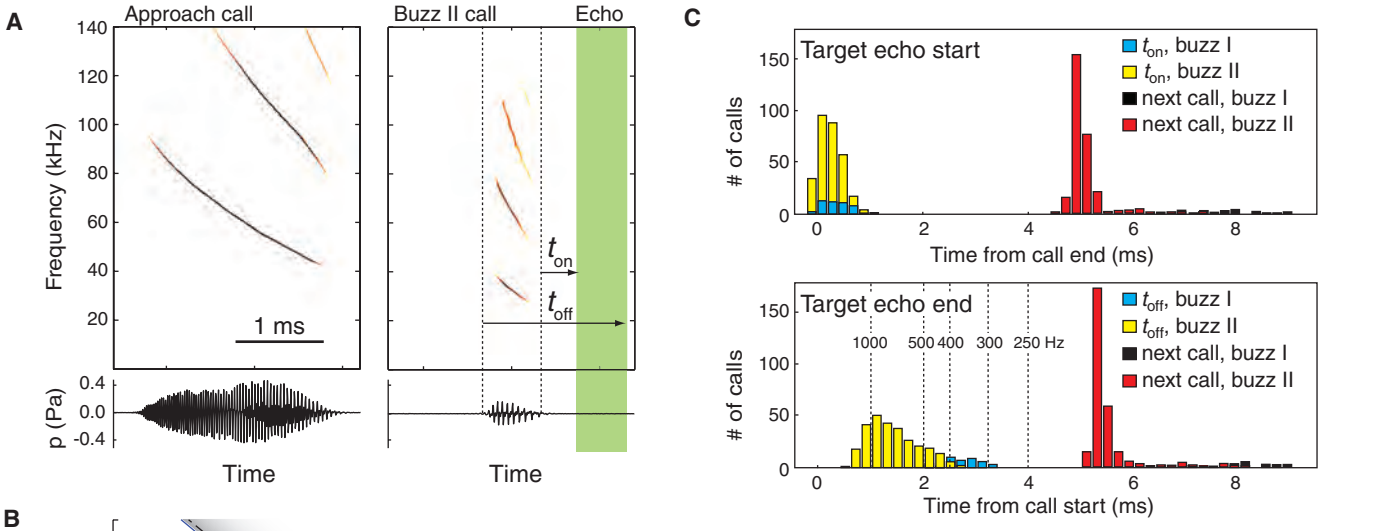

Fig. 2. Call-echo matching ambiguity does not limit echolocation call repetition rate. (**A**) High-frequency–time-resolution representation (*28*) and oscillogram of an approach and buzz II call showing smooth frequency sweeps. We calculated the time needed for the returning prey echo to reach the bat's ears (*10*) and quantified call duration, the time from call offset to echo onset (t_{on}), and the time from call onset to echo offset (t_{off}) for each call. (**B**) Call duration versus distance to prey. Call duration decreases during the buzz down to ~200 μs. Exemplary traces of five bats are shown (cyan circles, buzz I; red circles, buzz II). Call-echo overlap occurs when call duration exceeds the time needed for sound to travel to and from the prey calculated (i) solely based on call duration (dashed black line) and (ii) after adjusting for bat flight speed (blue line). (**C**) Histograms of t_{on} and t_{off} (cyan bars, buzz I; yellow bars, buzz II) in relation to the next call (black bars, buzz I; red bars, buzz II) for a total of 432 calls from four approaches per bat from five bats. Prey echoes start (top) and end (bottom) at the bat's ear well before the next call is produced. Vertical dotted lines indicate periods of higher repetition rates.

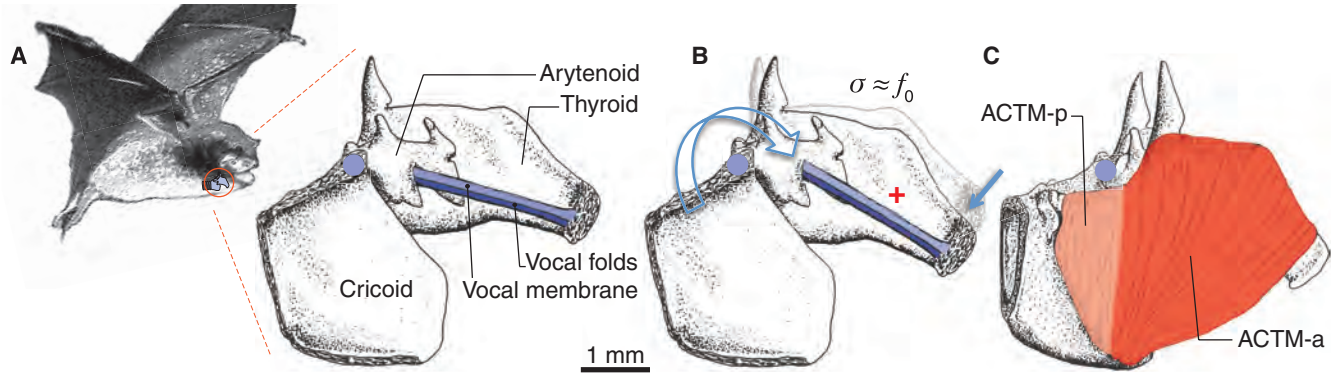

Fig. 3. Sound frequency modulation during echolocation calls. (**A**) Proposed frequency control mechanism of echolocation calls illustrated in schematic representation of a vespertilionid bat larynx [adapted from (*7*) with permission from R. A. Suthers]. Flow-induced self-sustained oscillations of the vocal folds (dark blue) and vocal membranes (light blue) generate ultrasonic pressure fluctuations. Their tension (σ) determines the fundamental frequency (f_0) of self-sustained oscillations. (**B**) Rotation (blue arrows) of the thyroid cartilage around the cricothyroid joint (blue circle) causes the vocal folds and membranes to stretch and adduct while the arytenoid cartilage remains stationary (*7*). This rotation increases fold and membrane length and tension (red plus) and thereby increases the fundamental frequency of produced sound. (**C**) The anterior cricothyroid muscle (ACTM) controls cricothyroid rotation and consists of an anterior (ACTM-a) and posterior part (ACTM-p). Relaxation of the ACTM-a results in f_0 decrease during phonation.

of several other laryngeal muscles controlling call duration are under debate (*6*, *7*, *13*). Because each echolocation call is under active neuromuscular control (*6*, *7*), call repetition rates >100 calls/s require separate work-producing cycles of muscle contraction and relaxation at the same rate. Contraction cycles this fast lie outside the capability of typical vertebrate synchronous skeletal muscle (*15*), which suggests that bat laryngeal muscles may be part of a rare group of superfast muscles, defined here as muscles capable of producing work >100 Hz. Such muscles have only ever been identified in the sound-producing organs of toadfish (*15*, *16*), rattlesnakes (*15*, *16*), and birds (*17*, *18*).

For the precise control of the terminal buzz, the main frequency modulating muscle must produce work and power at the repetition rates observed for the buzz (≤190 Hz) (Fig. 1). We conducted isometric twitch experiments on isolated muscle fibers of the main frequency modulating muscle (i.e., the anterior part of the anterior cricothyroid muscle) (Fig. 3C), which confirmed fast-twitch kinetics (Fig. 4A) and thus provided a necessary, but not sufficient, test of superfast muscle functionality (*15*). Twitch half-times measured 4.72 ± 0.38 ms at 39°C (N = 11 preparations from 7 individuals), faster than toadfish superfast swim-bladder muscle (5.8 ms at 25°C) (*16*) but slower than songbird superfast syringeal muscle (3.23 ms at 40°C) (*17*). The total contraction time was 8.27 ms during field stimulation of muscle fibers (*10*), almost twice as fast as the 12 to 16 ms reported for an anaesthetized big brown bat (*Eptesicus fuscus*, Vespertilionidae) in response to motor-nerve stimulation (*13*).

To demonstrate that superfast muscles are responsible for bats' ability to produce the buzz, we measured the mechanical performance of isolated bundles of muscle fibers by subjecting them to various strain cycles and stimulation regimes, that is, the work-loop technique (*10*). We found that bat laryngeal muscle produces both positive power and work at cycle frequencies up to 180 Hz and, in one case, up to 200 Hz (Fig. 4, B to D). At cycle frequencies of >180 Hz, the work loops deform to a figure-of-eight configuration (Fig. 4B). Beyond this point, negative work (Fig. 4B) starts to counteract the positive work in each loop. Above 200 Hz, negative work outweighs positive work, resulting in a negative net amount of work and power for all preparations. Thus, despite their extreme performance, Daubenton's bats' superfast laryngeal muscles perform up to, but not beyond, the cycle frequencies observed at the highest call rates in the buzz. Superfast muscles therefore allow, but limit, the maximum rate of bat echolocation call production.

Superfast muscles have been previously reported in a small number of species of reptiles, birds, and ray-finned fishes (*15*–*20*). We can now add mammals to that list. Studies of superfast synchronous muscle in nonmammalian species, most notably the oyster toadfish (*Opsanus tau*), indicate several hallmark adaptations to the basic contractile architecture (*15*, *19*, *20*) that allow for extremely rapid kinetics at every step in excitation-contraction coupling and relaxation. Histological studies of bat laryngeal muscle have revealed some similar modifications, including increased sarcoplasmic reticulum (*21*) and mitochondrial density (*22*). Intriguingly, the laryngeal and extraocular muscles of rats and rabbits express the myosin heavy-chain isoform MYH13 (*23*, *24*), which exhibits detachment rates from actin faster than is typical of skeletal muscles (*25*) and belongs to an ancient cluster of myosin genes (*26*). Whether similar isoforms are expressed in laryngeal echolocating bats remains to be seen.

We propose that the development of superfast muscles was crucial to the success of bats as aerial predators. Two innovations—powered flight and echolocation—are thought to have allowed bats to exploit the previously unrealized foraging niche of night-flying insects (*1*–*4*). Although a number of other vertebrates use echolocation for orientation (e.g., oilbirds, cave swiftlets, and a few tongue-clicking *Rousettus* spp. from the otherwise nonecholocating Old World fruit bats), only toothed whales and laryngeal echolocating bats use echolocation to detect prey, and only these animals produce buzzes (*27*). The ubiquity of buzzes in today's aerial hawking bats when taking prey (*1*, *2*, *9*) suggests that the capacity to emit short echolocation calls at very high rates evolved to enhance bats' success in capturing night-flying insects. We suggest that the demands of an active sensory system specialized for target acquisition, rather than simply orientation, selected for functional superfast vocal muscles needed to power the terminal buzz.

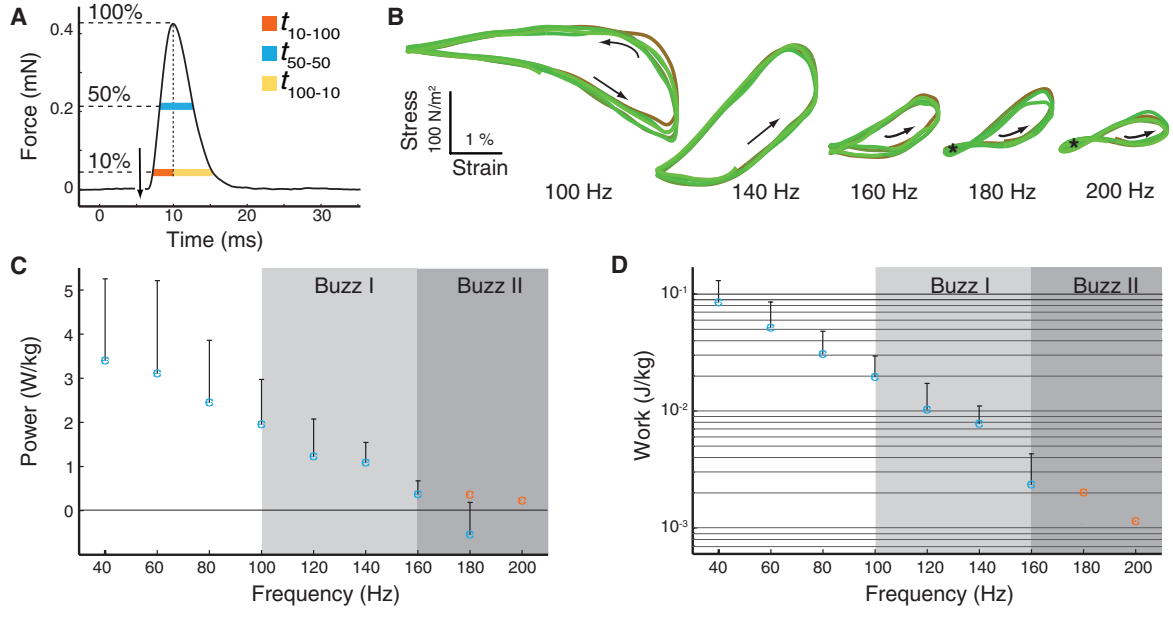

Fig. 4. Superfast performance of bat vocal muscle. (**A**) Isometric twitch recordings of ACTM-a preparations in vitro show extremely fast rise and decay times of 2.13 ± 0.33 ms (10 to 100% tension; N = 11 preparations from 7 individuals) and 6.14 ± 0.66 ms (100 to 10% tension), respectively. Downward arrow indicates stimulus. (**B**) Work-loop traces (five successive loops superimposed) of a preparation performing at cycle frequencies of 100, 140, 160, 180, and 200 Hz. At 180 and 200 Hz, increasing amounts of negative work appear (areas enclosed by clockwise rotation; asterisks) that counteract the production of positive work (areas enclosed by counterclockwise rotation) in each work loop. (**C**) Both power and (**D**) work (mean + SD) demonstrate that the anterior cricothyroid muscle is capable of producing positive power and work during cyclic contractions up to 160 Hz, and in one case up to 200 Hz. Orange dots indicate performance of the preparation depicted in (B).

References and Notes

1. H.-U. Schnitzler, E. K. V. Kalko, *Bioscience* **51**, 557 (2001).
2. J. M. Ratcliffe, in *Cognitive Ecology II*, R. Dukas, J. M. Ratcliffe, Eds. (Univ. Chicago Press, Chicago, 2009), pp. 201–225.
3. G. Jones, E. C. Teeling, *Trends Ecol. Evol.* **21**, 149 (2006).
4. D. R. Griffin, *Listening in the Dark* (Yale Univ. Press, New Haven, CT, 1958).
5. E. K. V. Kalko, H.-U. Schnitzler, *Behav. Ecol. Sociobiol.* **24**, 225 (1989).
6. R. A. Suthers, J. M. Fattu, *J. Comp. Physiol. A* **145**, 529 (1982).
7. G. E. Durant, thesis, Indiana University (1988).
8. S. Hiryu, M. E. Bates, J. A. Simmons, H. Riquimaroux, *Proc. Natl. Acad. Sci. U.S.A.* **107**, 7048 (2010).
9. L. Jakobsen, A. Surlykke, *Proc. Natl. Acad. Sci. U.S.A.* **107**, 13930 (2010).
10. Materials and methods are available as supporting material on *Science* Online.
11. P. A. Saillant, J. A. Simmons, F. H. Bouffard, D. N. Lee, S. P. Dear, *J. Acoust. Soc. Am.* **121**, 3001 (2007).
12. K. Ghose, T. K. Horiuchi, P. S. Krishnaprasad, C. F. Moss, *PLoS Biol.* **4**, e108 (2006).
13. R. A. Suthers, J. M. Fattu, *Am. Zool.* **13**, 1215 (1973).
14. W. Metzner, G. Schuller, in *Handbook of Mammalian Vocalization: An Integrative Neuroscience Approach*, S. M. Brudzynski, Ed. (Elsevier, Amsterdam, 2010), pp. 403–415.
15. L. C. Rome, *Annu. Rev. Physiol.* **68**, 193 (2006).
16. L. C. Rome, D. A. Syme, S. Hollingworth, S. L. Lindstedt, S. M. Baylor, *Proc. Natl. Acad. Sci. U.S.A.* **93**, 8095 (1996).
17. C. P. H. Elemans, A. F. Mead, L. C. Rome, F. Goller, *PLoS ONE* **3**, e2581 (2008).
18. C. P. H. Elemans, I. L. Y. Spierts, U. K. Müller, J. L. Van Leeuwen, F. Goller, *Nature* **431**, 146 (2004).
19. L. C. Rome *et al.*, *Proc. Natl. Acad. Sci. U.S.A.* **96**, 5826 (1999).
20. L. C. Rome, S. L. Lindstedt, *News Physiol. Sci.* **13**, 261 (1998).
21. J. P. Revel, *J. Cell Biol.* **12**, 571 (1962).
22. J. F. Reger, *J. Ultrastruct. Res.* **63**, 275 (1978).
23. M. M. Briggs, F. Schachat, *J. Exp. Biol.* **203**, 2485 (2000).
24. J. F. Hoh, *Acta Physiol. Scand.* **183**, 133 (2005).
25. Z. B. Li, G. H. Rossmanith, J. F. Y. Hoh, *Invest. Ophthalmol. Vis. Sci.* **41**, 3770 (2000).
26. B. T. Nasipak, D. B. Kelley, *Dev. Genes Evol.* **218**, 389 (2008).
27. J. A. Thomas, C. F. Moss, M. A. Vater, Eds., *Echolocation in Bats and Dolphins* (Univ. Chicago Press, Chicago, 2004).
28. T. J. Gardner, M. O. Magnasco, *Proc. Natl. Acad. Sci. U.S.A.* **103**, 6094 (2006).

Acknowledgments: We thank R. Suthers for permission to reprint Fig. 3 from (*7*); R. Langill, P. Martensen, and F. Mortensen for technical assistance; G. Lutz for providing carbon microspheres; T. Gardner for sparse time-frequency Matlab scripts; and F. Jensen, D. Canfield, A. Surlykke, and A. West for use of equipment. F. Andrade, S. Brinkløv, P. Faure, B. Fenton, B. Galef, J. van Leeuwen, P. Madsen, M. Nydam, A. Surlykke, H. ter Hofstede, and S. Zawadzki commented on the manuscript. This study was funded by grants from the Danish Research Council (FNU), Carlsberg Foundation, and Grass Foundation to C.P.H.E.; Company of Biologists to A.F.M.; Oticon Foundation to L.J.; and FNU to J.M.R. Animal capture and experimentation was approved by Skov- og Naturstyrelsen (Denmark). C.P.H.E. and J.M.R. conceived of the study. C.P.H.E. and A.F.M. conducted physiological experiments; C.P.H.E., L.J., and J.M.R. conducted behavioral experiments. All authors contributed to data analysis. C.P.H.E. and J.M.R. wrote the manuscript. The data reported in this paper are available from C.P.H.E and J.M.R.

Supporting Online Material

www.sciencemag.org/cgi/content/full/333/6051/1885/DC1
Materials and Methods
Fig. S1
References

21 April 2011; accepted 15 August 2011
10.1126/science.1207309

An Expanded Palette of Genetically Encoded Ca^{2+} Indicators

Yongxin Zhao,[1] Satoko Araki,[2] Jiahui Wu,[1] Takayuki Teramoto,[3] Yu-Fen Chang,[2] Masahiro Nakano,[2] Ahmed S. Abdelfattah,[1] Manabi Fujiwara,[3] Takeshi Ishihara,[3] Takeharu Nagai,[2,4] Robert E. Campbell[1]*

Engineered fluorescent protein (FP) chimeras that modulate their fluorescence in response to changes in calcium ion (Ca^{2+}) concentration are powerful tools for visualizing intracellular signaling activity. However, despite a decade of availability, the palette of single FP-based Ca^{2+} indicators has remained limited to a single green hue. We have expanded this palette by developing blue, improved green, and red intensiometric indicators, as well as an emission ratiometric indicator with an 11,000% ratio change. This series enables improved single-color Ca^{2+} imaging in neurons and transgenic *Caenorhabditis elegans*. In HeLa cells, Ca^{2+} was imaged in three subcellular compartments, and, in conjunction with a cyan FP–yellow FP–based indicator, Ca^{2+} and adenosine 5′-triphosphate were simultaneously imaged. This palette of indicators paints the way to a colorful new era of Ca^{2+} imaging.

Fluorescent indicators for the quantification of intracellular Ca^{2+} have been indispensable tools of cell biology for three decades (*1*), yet the need for new indicators has continued to grow as advances in molecular biology and microscopy instrumentation reveal the limitations of each previous generation. Accordingly, there has been a push toward Ca^{2+} indicators that are longer wavelength, ratiometric, and higher signal-to-noise, and—since the advent of green fluorescent protein (GFP)—genetically encodable. A ratiometric indicator excites or emits at distinct wavelengths in the Ca^{2+}-free and Ca^{2+}-bound states and provides the advantages of being quantitative and less susceptible to imaging artifacts. Two important classes of genetically encoded Ca^{2+} indicators are the Förster resonance energy transfer (FRET)–based cameleon type (*2*), and the single GFP type, such as GCaMP (*3*) and flash-pericam (*4*), that are dim in the absence of Ca^{2+} and bright when bound to Ca^{2+}. GCaMPs are composed of a circularly permuted (cp) GFP fused to the calmodulin (CaM)–binding region of chicken myosin light chain kinase (M13) at its N terminus and a vertebrate CaM at its C terminus. Binding of Ca^{2+} causes the M13 and CaM domains to interact and the interface between CaM and the fluorescent protein (FP) to reorganize, which leads to an increase in fluorescence due to water-mediated interactions between the chromophore and R377 (*5*) of CaM (*6*, *7*).

Although directed protein evolution has provided many improved FPs, it has not proven particularly effective for the production of improved GCaMPs. Directed evolution of FPs is typically guided by digital fluorescence imaging of large libraries of gene variants expressed in *Escherichia coli* colonies. In this manner, rare clones that harbor a mutation that confers a desirable trait, such as improved brightness or altered hue, can be identified in libraries of $>10^5$ variants. Lacking an analogous screen for GCaMP Ca^{2+} response, researchers have identified improved variants by manual testing (*7*, *8*) and a medium-throughput cell-based assay (*9*).

To accelerate the development of improved and hue-shifted GCaMP-type indicators, we developed a colony-based screen for Ca^{2+}-dependent fluorescent changes (Fig. 1) [supporting online material (SOM) text]. The premise of this screening system is that Ca^{2+} indicators targeted to the *E. coli* periplasm can be shifted toward the Ca^{2+}-free or Ca^{2+}-bound states by experimental manipulation of the environmental Ca^{2+} concentration. Accordingly, screening of large libraries of genetic variants of GCaMP-type indicators can be achieved by digital fluorescence imaging, at both high- and low-Ca^{2+} conditions, of plates containing hundreds of *E. coli* colonies each. We used this screening system to undertake a process of directed evolution that explored the sequence space accessible from the most optimized single FP Ca^{2+} indicator, GCaMP3 (*9*). Initially, we created a large library by error-prone polymerase chain reaction (PCR) and screened $\sim 2 \times 10^5$ colonies to identify the offspring with the largest Ca^{2+}-dependent changes in green fluorescence (*10*). After this and subsequent iterative rounds of library creation and screening

[1]Department of Chemistry, University of Alberta, Edmonton, Alberta T6G 2G2, Canada. [2]Research Institute for Electronic Science, Hokkaido University, Kita 20, Nishi 10 Kita-ku, Sapporo 001-0020, Japan. [3]Department of Biology, Faculty of Sciences, Kyushu University, 6-10-1, Hakozaki, Higashi-ku, Fukuoka, 812-8581, Japan. [4]PRESTO, Japan Science and Technology Agency, 5 Sanbancho, Chiyoda-ku, Tokyo 102-0075, Japan.

*To whom correspondence should be addressed. E-mail: robert.e.campbell@ualberta.ca

www.sciencemag.org/cgi/content/full/333/6051/1885/DC1

Supporting Online Material for

Superfast Muscles Set Maximum Call Rate in Echolocating Bats

Coen P. H. Elemans,* Andrew F. Mead, Lasse Jakobsen, John M. Ratcliffe*

*To whom correspondence should be addressed.
E-mail: coen@biology.sdu.dk (C.P.H.E.); jmr@biology.sdu.dk (J.M.R.)

Published 30 September 2011, *Science* **333**, 1885 (2011)
DOI: 10.1126/science.1207309

This PDF file includes:

Materials and Methods

Echolocation and flight path reconstruction

We recorded echolocation calls during a bat's attack on a suspended mealworm (5 bats, 4 sequences/bat) using an array of 12 quarter-inch G.R.A.S. microphones arranged and sampled as described elsewhere (*9*). For each sequence, the bat's position was estimated at each call emission by triangulation of the differences in arrival times at the 12 microphones. We derived flight path kinematics from positioning information. Call duration was measured from the channel recording the highest intensity and defined as time segments containing sound-pressure ≥2 times background noise level. For each call, the prey echo arrival at the bat's ears was calculated as the time needed for sound to travel to and from the target, corrected for bat displacement. We calculated the duration of prey echoes returning from a single call as each call's measured duration plus the duration of reverberating sound waves reflecting from a fictive prey insect measuring 5 cm in line with the sound wave direction. The onset of all returning echoes related to the prey is calculated as the time needed for the sound wave travelling back and forth from the bat to the closest part of the prey measured from the start of a call. The echo offset is calculated as the time needed for the sound wave travelling back and forth from the bat to the furthest part of the prey measured from the end of a call, also taking into account the position change of the bat during flight.

Laryngeal muscle physiology

We measured work output and power performance of isolated bundles of laryngeal muscle using the work-loop technique *(17)* with a setup adapted to superfast performance. In this technique, isolated whole muscles or bundles of fibers are stimulated electrically while being forced through cyclical length changes to quantify the amount of work and power they produce. For detailed descriptions of concepts and protocols see (*17*). Small strips of the anterior portion of the anterior cricothyroid muscle from the larynxes of eight *Myotis daubentonii* were isolated and connected to a high-speed servomotor (model 322, Aurora Scientific) and force transducer (model 400A, Aurora Scientific) using 10/0 silk suture. The bath in which the tissue was immersed was kept at 39°C (± 0.1°C) using PID controlled (E5CN, Omron) Peltier elements and continuously perfused with oxygenated Ringer's solution (NaCl, 154; KCl, 6; $MgCl_2$, 1; $CaCl_2$, 4; NaH_2PO_4, 1; $MgSO_4$, 1; hepes, 10; glucose, 12; pH adjusted to 7.4 with Trizma base

[mmol/l]). The fibers measured 1.86 ± 0.25 mm (N=11) at resting length and were electrically stimulated with platinum electrodes using a follow stimulator (model 701C, Aurora Scientific). As previously observed in superfast muscles (*19*), tension trades-off for speed and the maximum isometric stress during single twitch contraction measured only 4.7 ± 3.9 kN/m^2. To quantify and correct for any strain deviation from the imposed strain by the servo motor, we measured strain optically by filming carbon beads (50 µm diameter) stuck to the fibers at 20 kHz using a high-speed camera (HS4, Redlake) mounted on a stereomicroscope (M165-FC, Leica microsystems). All control and analysis software was written in Matlab. Animal capture was approved by Skov- og Naturstyrelsen (Denmark) and all experiments were conducted in accordance with the animal care and use committee of the University of Southern Denmark.

Figure S1.

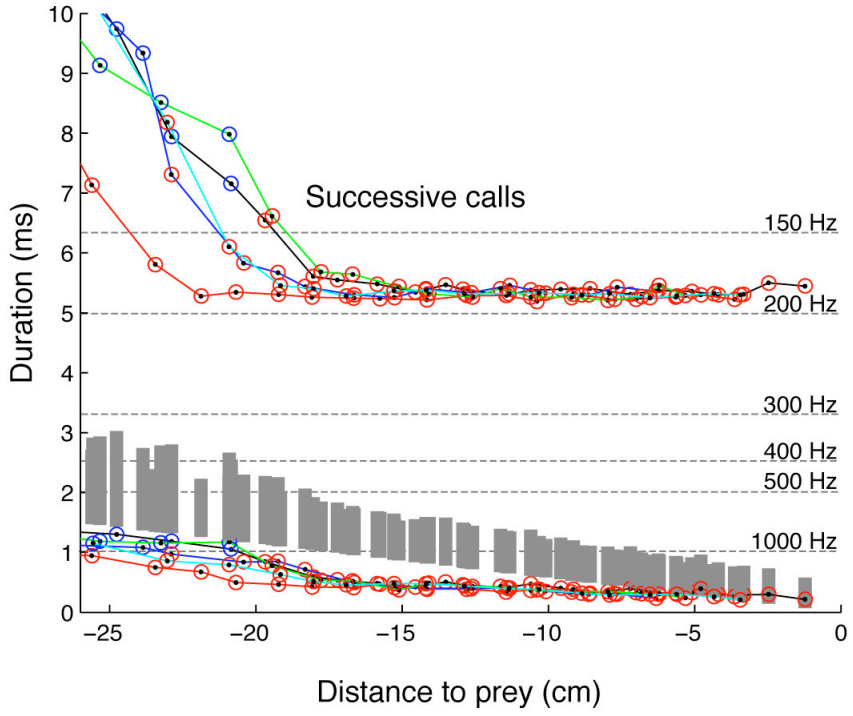

Timing of echo arrival at the bats' ears during attack sequences.

Exemplary attack sequences from each of the five bats are shown. Traces of call duration versus prey distance are shown in bottom of graph (different colour used for each of the five bats, blue circles, buzz I; red circles, buzz II). The vertical grey bars indicate the timing and duration of the target echoes from each of these calls. The top traces indicate the timing of the successive echolocation call during the attack sequence. The horizontal dotted lines indicate potential call repetition rates at the corresponding call periods. These data show that echoes never overlap or surpass the next call emitted, avoiding echo to call matching ambiguity. For all calls in buzz II, call repetition rate could be as high as 400 calls/sec without call-echo matching ambiguity, two times higher than the 190 calls/sec observed in the buzz. Call repetition rate could be increased more over the course of an attack before echo-next call overlap would become problematic: up to 500 calls/sec for 91% of the calls, and 800 calls/sec for 54% of the 346 calls recorded during 4 attack sequences from each of 5 bats (Fig. 2C). Therefore call-echo ambiguity does not limit echolocation call repetition rate.

References

1. H.-U. Schnitzler, E. K. V. Kalko, *Bioscience* **51**, 557 (2001).

2. J. M. Ratcliffe, in *Cognitive Ecology II*, R. Dukas, J. M. Ratcliffe, Eds. (Univ. Chicago Press, Chicago, 2009), pp. 201–225.

3. G. Jones, E. C. Teeling, *Trends Ecol. Evol.* **21**, 149 (2006).

4. D. R. Griffin, *Listening in the Dark* (Yale Univ. Press, New Haven, CT, 1958).

5. E. K. V. Kalko, H.-U. Schnitzler, *Behav. Ecol. Sociobiol.* **24**, 225 (1989).

6. R. A. Suthers, J. M. Fattu, *Eptesicus. J. Comp. Physiol. A* **145**, 529 (1982).

7. G. E. Durant, Laryngeal control of the duration and frequency of emitted sonar pulses in the echolocating bat, *Eptesicus fuscus* (PhD thesis, Indiana University, 1988).

8. S. Hiryu, M. E. Bates, J. A. Simmons, H. Riquimaroux, *Proc. Natl. Acad. Sci. U.S.A.* **107**, 7048 (2010).

9. L. Jakobsen, A. Surlykke, *Proc. Natl. Acad. Sci. U.S.A.* **107**, 13930 (2010).

10. Materials and methods are available as supporting material on *Science* Online.

11. P. A. Saillant, J. A. Simmons, F. H. Bouffard, D. N. Lee, S. P. Dear, *J. Acoust. Soc. Am.* **121**, 3001 (2007).

12. K. Ghose, T. K. Horiuchi, P. S. Krishnaprasad, C. F. Moss, *PLoS Biol.* **4**, e108 (2006).

13. R. A. Suthers, J. M. Fattu, *Am. Zool.* **13**, 1215 (1973).

14. W. Metzner, G. Schuller, in *Handbook of Mammalian Vocalization: An Integrative Neuroscience Approach*, S. M. Brudzynski, Ed. (Elsevier, Amsterdam, 2010), pp. 403–415.

15. L. C. Rome, *Annu. Rev. Physiol.* **68**, 193 (2006).

16. L. C. Rome, D. A. Syme, S. Hollingworth, S. L. Lindstedt, S. M. Baylor, *Proc. Natl. Acad. Sci. U.S.A.* **93**, 8095 (1996).

17. C. P. H. Elemans, A. F. Mead, L. C. Rome, F. Goller, *PLoS ONE* **3**, e2581 (2008).

18. C. P. H. Elemans, I. L. Y. Spierts, U. K. Müller, J. L. Van Leeuwen, F. Goller, *Nature* **431**, 146 (2004).

19. L. C. Rome *et al*., *Proc. Natl. Acad. Sci. U.S.A.* **96**, 5826 (1999).

20. L. C. Rome, S. L. Lindstedt, *News Physiol. Sci.* **13**, 261 (1998).

21. J. P. Revel, *J. Cell Biol.* **12**, 571 (1962).

22. J. F. Reger, *J. Ultrastruct. Res.* **63**, 275 (1978).

23. M. M. Briggs, F. Schachat, *J. Exp. Biol.* **203**, 2485 (2000).

24. J. F. Hoh, *Acta Physiol. Scand.* **183**, 133 (2005).

25. Z. B. Li, G. H. Rossmanith, J. F. Y. Hoh, *Invest. Ophthalmol. Vis. Sci.* **41**, 3770 (2000).

26. B. T. Nasipak, D. B. Kelley, *Dev. Genes Evol.* **218**, 389 (2008).

27. J. A. Thomas, C. F. Moss, M. A. Vater, Eds., *Echolocation in Bats and Dolphins* (Univ. Chicago Press, Chicago, 2004).

28. T. J. Gardner, M. O. Magnasco, *Proc. Natl. Acad. Sci. U.S.A.* **103**, 6094 (2006).